Pergamon

Geochimica et Cosmochimica Acta, Vol. 67, No. 5, pp. 807–812, 2003

0016-7037/03 $30.00 + .00

PII S0016-7037(00)00923-7

Characterization of the structure and the surface reactivity of a marcasite thin film

ALICIA R. ELSETINOW,[1] DANIEL R. STRONGIN,[1,*] MICHAEL J. BORDA,[2] MARTIN A. SCHOONEN[2] and KEVIN M. ROSSO[3]

[1]Chemistry Department, Temple University, Philadelphia, PA 19122, USA
[2]Geosciences Department, State University of New York at Stony Brook, Stony Brook, NY 11780, USA
[3]W. R. Wiley Environmental Molecular Sciences Laboratory, Pacific Northwest National Laboratory, PO Box 999, MSIN K8-96, Richland, WA 99352, USA

(*Received November* 15, 2001; *accepted in revised form April* 5, 2002)

Abstract—A thin film of marcasite, FeS_2, was synthesized under vacuum and its structure and reactivity under oxidizing conditions was investigated by means of diffraction and surface analytical techniques, respectively. Synthesis of the film was carried out by codepositing Fe and S_2 onto a Ta support. The thickness of the film could be varied from approximately 10 Å to 1 μm. High-resolution S 2p synchrotron-based photoemission showed S_2^{2-}, with undetectable amounts of S^{2-} impurity that is typically present on natural sample surfaces. X-ray diffraction of the micron-thick films showed that the film crystallized in the marcasite phase of FeS_2. Atomic force microscopy indicated that the thin film had a nanometer-scale roughness suggesting the film contained defects such as steps and kinks. X-ray photoelectron spectroscopy studies found the thin marcasite film to be more reactive than natural pyrite (the most ubiquitous FeS_2 dimorph) after exposure to a gaseous O_2/H_2O environment on the basis of the amount of sulfate formation. Likely the oxidation of marcasite was dominated by its short-range order (e.g., presence of steps), because the density of nonstoichiometric defect sites (e.g., S^{2-}) was low as assessed by photoelectron spectroscopy.

1. INTRODUCTION

The synthesis and subsequent study of well-defined thin films of metals and their oxides have often led to a better understanding of a specific material of interest than could be obtained by studying the associated bulk material (Chusuei et al., 2001). An excellent example of the contribution of thin films as a model substrate for a more complicated bulk material is in the area of catalysis. Thin films have been instrumental in developing a framework by which to understand the surface properties of metals, metal oxides, metal sulfides, and alloys as catalytic supports, catalysts, or both (Somorjai, 1994; Freund et al., 2001). The controlled conditions under which thin films are produced commonly allow better characterization of surface properties than can be achieved on fractured or cleaved surfaces. These properties include surface reactivity, electronic structure, and geometric surface structure (Rodriguez and Goodman, 1995). Furthermore, the growth of thin insulating films (often metal oxides) on conducting substrates can alleviate sample charging that is problematic when studying bulk-insulating materials (St. Clair and Goodman, 2000). This is also a common problem with regard to surface studies of minerals.

Environmentally important minerals are not always conducive to surface science investigations as a result of complex topographies, ill-defined surface structures, insulating properties, or some combination of these. Furthermore, natural minerals often contain impurity atoms, which complicate studies of the intrinsic properties of the mineral and its surface. Toward developing a better understanding of the interaction of minerals with the environment, there has been a significant effort in the growth of thin films, as well as in the analysis and modeling of prepared surfaces. In the case of metal oxide minerals, for example, extensive research has been concerned with the growth of well-defined thin model iron oxide surfaces (Kim et al., 1999; Thevuthasan et al., 1999; Chambers, 2000; Chambers et al., 2000) for surface analytical studies of an environmental nature. The growth of metal sulfide thin film surfaces, which is the focus of this contribution, has also received significant attention. The motivation for generating these surfaces, however, has generally been for their materials properties, rather than for surface analytical studies of their interactions with environmentally relevant adsorbates. For example, the growth of pyrite, FeS_2 thin films, have received significant attention as a result of its potential photoelectric properties (Ennaoui et al., 1993; Thomas et al., 1995, 1997), not because of its profound role in controlling chemistry in the environment.

The motivation for the present study is to investigate marcasite (a dimorph of pyrite) reactivity in an oxidizing environment. The degradation of marcasite in oxidizing atmospheres plays a role in acid mine drainage. The study of a thin film of marcasite is particularly attractive because natural marcasite samples have a complicated morphology, making it difficult to obtain reproducible surfaces. In contrast, natural samples of its dimorph, pyrite, can be readily obtained that are conducive to surface science studies (Elsetinow et al., 2000). Previous studies have investigated the growth of marcasite thin films by chemical vapor deposition (Hoepfner et al., 1995; Meester et al., 2000) and molecular beam (Bronold et al., 1997) techniques, but have not studied the reactivity of the thin films.

In the present study, a thin film of marcasite ($<1\mu$m) was characterized by X-ray diffraction (XRD), atomic force microscopy (AFM), and high-resolution X-ray photoelectron spectroscopy (XPS). Thin film growth was carried out in the vacuum environment by the codeposition of Fe and S_2 gas (provided by an electrochemical cell). The reactivity of the marcasite film

* Author to whom correspondence should be addressed (dstrongi@nimbus.ocis.temple.edu).

was investigated after exposure to a gaseous H_2O/O_2 environment (supported on a Ta foil) with XPS. The synthetic approach outlined in this contribution may be more conducive to growth in a vacuum surface science chamber than prior synthetic routes.

2. EXPERIMENTAL METHODS

Experimental results presented in this contribution were obtained at four different locations. XPS reactivity studies of the marcasite thin film were carried out at Temple University, high-resolution photoelectron spectroscopy was performed in the U7A end station at the National Synchrotron Light Source (NSLS) at Brookhaven National Laboratory, AFM experiments were carried out at Pacific Northwest National Laboratory, and XRD measurements were performed at the State University of New York at Stony Brook.

2.1. Photoelectron Spectroscopy

Fe and S 2p XPS data were obtained with Mg-Kα (1253.6 eV) radiation and a double-pass cylindrical mirror analyzer at a pass energy of 25 eV. The spectrometer was calibrated by using the 4f, 4d, and 4p peaks of a gold single crystal. Photoelectron data at the NSLS were obtained with 240 eV photons and a 250-mm hemispherical analyzer (pass energy of 22 eV). All the binding energies are referenced to the Fermi level, E_F. The position of E_F was obtained by determining the energy position of the photoelectron cutoff in the valence band region of a freshly deposited metallic Fe film.

2.2. Thin Film Growth

Thin marcasite films were grown on a Ta foil in an ultrahigh vacuum (UHV, 1×10^{-9} torr) chamber. Thin films investigated by XPS and AFM were grown at Temple University in an integrated UHV–high-pressure reaction cell facility, which has been described previously (Guevremont et al., 1998b). High-resolution photoelectron spectroscopy was carried out on a thin film grown in situ at the NSLS.

In both locations, film growth was carried out in a UHV chamber by codepositing Fe and S_2 from the vapor phase. Fe vapor production was accomplished by resistively heating a tungsten wire that was wrapped with Fe wire. S_2 gas was generated by a Ag_2S electrochemical cell (Wagner, 1953) by using a design that has been described in detail by others (Heegeman et al., 1975; Hrbek et al., 1992).

Formation of the marcasite thin film was accomplished after several steps. Initially, the substrate was cooled to 200 K. S_2 was then condensed on the substrate while codepositing Fe to form layers of pure metal and sulfur with metalsulfide complexes at their interfaces. At this point, S 2p core level spectra showed several sulfur-derived features assigned to multilayer S_2 and S species in the 1− and 2− oxidation states, suggesting that condensed sulfur, FeS_2, and FeS were present. The sample was subsequently heated to 473 K in a background S_2 pressure of 10^{-5} to 10^{-4} torr. The sample was held at 473 K for approximately 2 min, after which the sample was allowed to cool to room temperature while maintaining the sulfur pressure.

The average thickness of each thin film was estimated on the basis of attenuation of the Ta substrate $4d_{5/2}$ signal. The kinetic energy of photoelectrons associated with the Ta peak was approximately 1028 eV (using Mg Kα radiation). Assuming that the mean free path of these photoelectrons are approximately 20 Å (Somorjai, 1981), the rate of the initial film growth could be determined. This rate was extrapolated to thicker films where the Ta photoelectron signals were completely attenuated and could not be used as a thickness indicator. It is emphasized that film thickness obtained by this method is only an estimate because film morphology will certainly affect this attenuation method.

Fig. 1 exhibits a wide XPS scan of the FeS_2 thin film (top). Within the experimental sensitivity of our XPS, there is no carbon or oxygen contamination, which is often intrinsic to natural sulfide samples that are used in surface science studies. As a comparison, a wide XPS scan of natural-crushed marcasite sample (bottom) is also exhibited. The as-received marcasite was cleaned with 0.5 mol/L HCl acid by means of a method used in our laboratory for {100} pyrite (Guevremont et al., 1998a) and introduced into the UHV chamber without exposure to air.

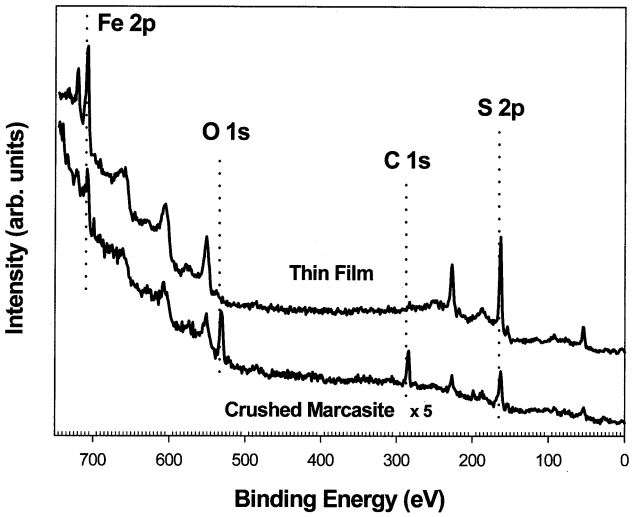

Fig. 1. XPS wide scan of the marcasite thin film (top) compared with a natural-crushed marcasite sample (bottom). Carbon and oxygen contamination, which is often intrinsic to natural sulfide minerals, is not present in the thin film.

In contrast to the thin film, the natural marcasite sample shows significant carbon and oxygen contamination. Furthermore, natural pyrite samples, for example, can contain trace impurities and mineral inclusions (Lodders et al., 1998). From experience in our laboratory, we find that vacuum-fractured pyrite always contains small but detectable amounts of oxygen, carbon, or both. This comparison brings to light a potential advantage of the thin film approach. Namely, the thin film can offer an atomically clean sample for surface science studies.

2.3. Thin Film Reactivity

For reactivity studies, thin films were exposed to a gaseous mixture composed of H_2O (0.02 bar) and O_2 (1 bar) in a high-pressure reaction cell. All exposures were carried out for 20 h, and at no time were the samples exposed to the ambient atmosphere of the laboratory.

2.4. Atomic Force Microscopy

Contact mode AFM was performed under ambient conditions with a Digital Instruments BioScope located at Pacific Northwest National Laboratory. A thin film sample grown on a Ta plate was transferred directly from vacuum into a sealed container under an N_2 atmosphere and shipped. Imaging was performed in air immediately after removing the sample from the sealed container and mounting in the AFM. Standard Si_3N_4 probes were used, having a nominal radius of curvature of 20 to 60 nm and an approximate spring constant of 0.12 N/m. Contact forces were minimized upon engagement. Images were also collected under air-equilibrated 18 MΩ water in an attempt to minimize noise possibly arising from capillary forces on the tip from adventitious water layers at the sample-tip contact. Image processing to remove piezo tilt and bow and sporadic noise where necessary, and image analyses were performed by the Digital Instruments software, version 4.23r5.

2.5. X-ray Diffraction

The structure of an FeS_2 film was determined by XRD. Experiments were performed on a Bruker AXS GADDS (General Area Detector Diffraction System) platform mounted with a XYZ-translating stage and a Bruker Hi-STAR detector. Cu Kα radiation was used with a graphite [111] monochromator to filter out Cu Kβ. The beam was collimated to 800 μm. A thin film of aluminum foil was placed directly in front of the Hi-STAR detector, covering the entire detector face, to limit the effect of iron fluorescence.

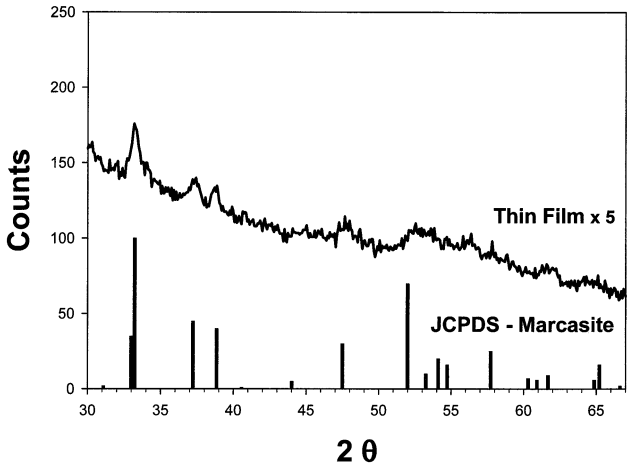

Fig. 2. XRD of a 1-μm-thick FeS_2 film formed by codepositing Fe and S_2 on a Ta foil in the vacuum environment. The diffraction data indicate that the FeS_2 grows in the marcasite structure, a finding that is based on the agreement with a powder diffraction standard for marcasite.

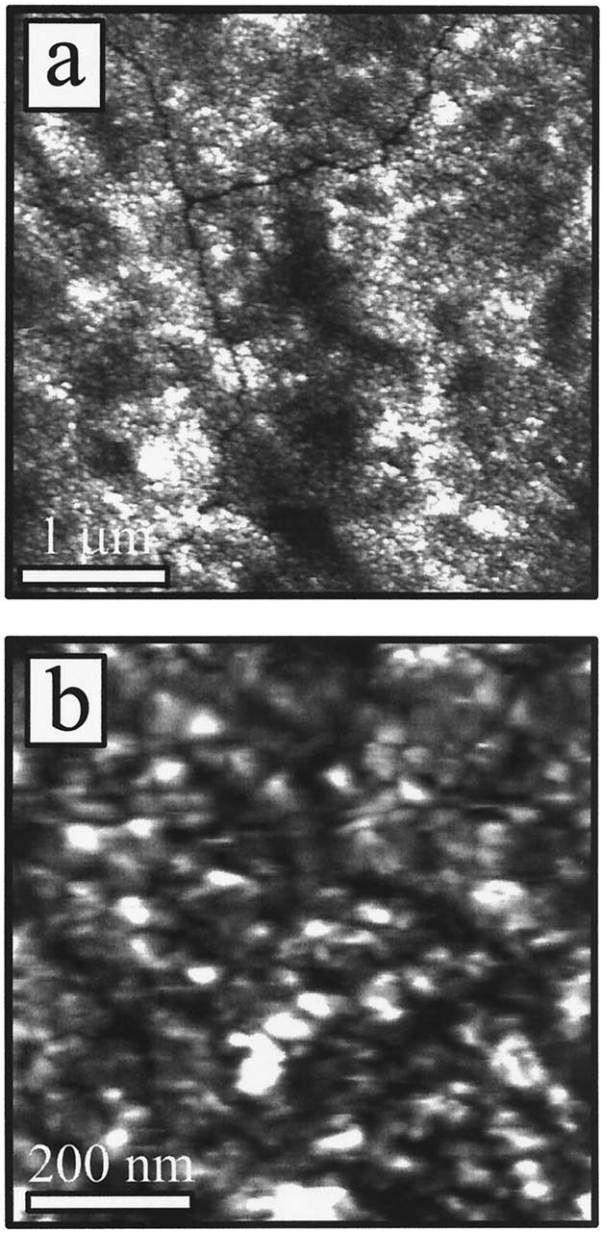

Fig. 3. Large- (a) and small- (b) scale AFM images showing the surface microtopography of a thin film sample. The height ranges for the images are 50 and 25 nm, respectively.

3. RESULTS AND DISCUSSION

3.1. Characterization of Thin Film

The primary assignment of the marcasite phase of FeS_2 to the thin film is based on XRD data shown in Figure 2. The diffraction pattern was consistent with the standard patterns for marcasite found in the JCPDS catalog.

AFM characterization indicated that the thin film was a uniform, finely textured coating (Fig. 3a) covering a relatively coarser microtopography associated with the Ta plate (data not shown). Fine randomly oriented fractures, of unknown origin, were observed at spatial separations of between 1 and 10 μm (Fig. 3a). No scouring was observed after repeated imaging over the same area.

Good AFM image quality was attained down to ~500 nm (Fig. 3b). At these scales, the surface topography associated with the thin film was isolated. No indication of surface oxidation was apparent during 1 h of scanning. Surface indulations (bumps) were found to have irregular shape and variable size. An root-mean-square (RMS) roughness analysis of the image in Figure 3b indicates that the standard deviation in height was 4.6 nm. Thus, the topographic relief associated with the thin film and the height of the surface features is approximately 10 nm. Grain size analysis of the features lying topographically above the mean height plane indicated that the average lateral area of each feature in the *x*, *y* plane is ~1400 nm^2, suggesting an average lateral radius of ~21 nm when approximated as circular. Therefore, the features have a height-to-width ratio of ~1:4. Power spectral density analyses of the periodicity in the *x*, *y* plane show a small spike at 70 to 80 nm spatial frequencies indicative of a somewhat regular lateral spacing between the features, but such regularities do not dominate the power spectrum.

The collective AFM observations reveal no obvious crystallographic control in the structure of the surface at the length scales achieved. This is, perhaps, not surprising because the film was grown on a polycrystalline substrate with unknown surface microtopography. However, the nanometer-scale roughness is suggestive of a high aerial density of surface sites such as steps and kinks occurring at smaller scales.

Photoelectron results obtained with synchrotron radiation add some microscopic insight with regard to the surface electronic structure of the film. Figure 4 displays high-resolution S 2p photoelectron spectroscopy of a marcasite thin film (thickness of ≈100 Å) and a pyrite sample that was cleaved in an inert atmosphere and then transferred to UHV. On the basis of previous work, the features in the S 2p spectrum for pyrite can be assigned to S_2^{2-} in the bulk (162.6 eV) and surface (162.1 eV), and S^{2-} impurity (161.3 eV). Recent research in another laboratory has obtained high-resolution S 2p data for cleaved

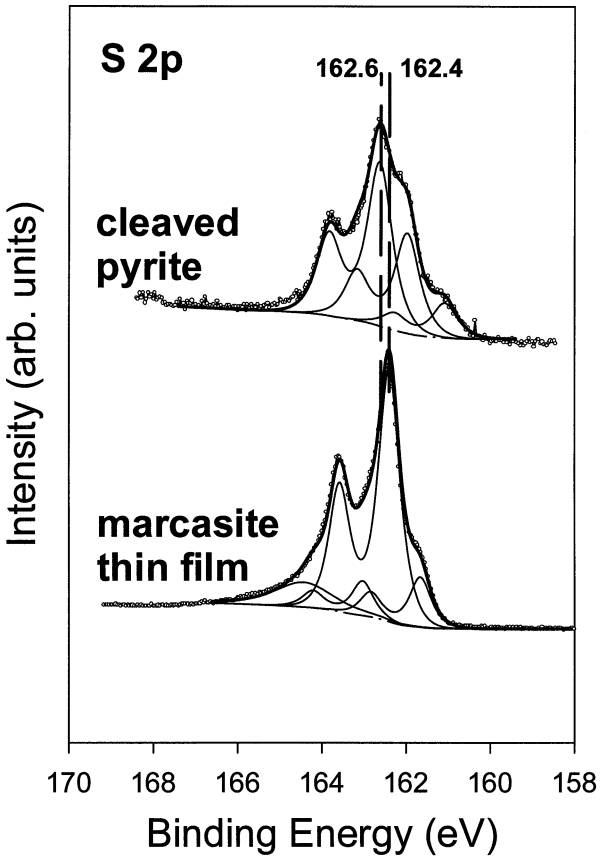

Fig. 4. High-resolution S 2p photoelectron spectroscopy of the thin film and of {100} pyrite that was cleaved in an inert atmosphere and then transferred to UHV. Dashed curves are fitted S 2p doublets (FWHM = 0.6 eV; splitting of 1.18 eV).

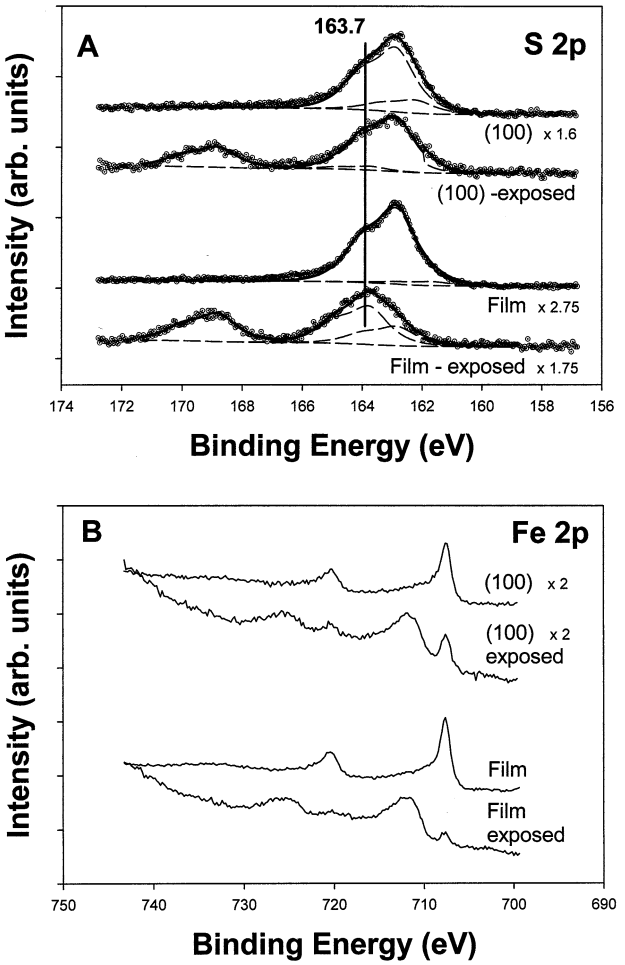

Fig. 5. XPS S 2p (a) and Fe 2p (b), respectively, for {100} pyrite and the marcasite thin film before and after 20-h exposure to a gaseous H_2O/O_2 environment (Fig. 5).

natural marcasite (Uhlig et al., 2001). The assignments in this previous study are generally consistent with pyrite, except for rather small binding energy shifts. For example, the S 2p feature for bulk and surface S_2^{2-} are at 162.5 and 161.9 eV, and the S^{2-} appeared at 161.4. The S 2p spectrum, however, unlike that obtained for pyrite contained significant intensity that was assigned to short chain polysulfides near 163 eV.

Inspection of the S 2p spectrum for the marcasite thin film shows some similarities, but also some differences with cleaved natural marcasite. First, the S 2p feature near 162.4 eV for the thin film can be readily assigned to the S_2^{2-} group of marcasite. Perhaps, there is somewhat more ambiguity in assigning the 161.7-eV feature. One interpretation is that this feature is due to the S^{2-} impurity species, where the peak in the thin film would lie ~0.3 eV above where S^{2-} appears in the natural marcasite spectrum (161.4 eV) (Uhlig et al., 2001). A more favored interpretation, however, is that the 161.7-eV feature is due to surface shifted S_2^{2-}. This assignment is in reasonable agreement with the assignment of surface shifted S_2^{2-} to a 161.9-eV feature in the S 2p spectrum of natural marcasite. Our assignments suggest that the marcasite film has no S^{2-} impurity (within our experimental resolution), in contrast to natural disulfide samples. This result is not completely unexpected because the preparation of natural pyrite or marcasite surfaces often relies on fracture, a preparative technique that might be expected to introduce nonstoichiometric sites.

Further inspection of the S 2p spectrum of the thin film shows S 2p intensity near 163 eV, which we assign to polysulfide species. The contribution of this feature is relatively small, accounting for ~5% of the integrated S 2p intensity. Cleaved natural marcasite exhibits a more significant feature associated with short-chained polysulfides near 163.2 eV. Although the origin of these features are presumably quite different for both types of marcasite samples, the comparison does suggest that the thin film contains significantly less polysulfide impurity than a freshly prepared natural marcasite sample.

3.2. Reactivity of Marcasite Film

Figure 5 a and b exhibit conventional XPS S 2p and Fe 2p spectra, respectively, for {100} pyrite and the marcasite film before and after a 20-h exposure to a gaseous H_2O/O_2 environment. S 2p data show that in both cases, exposure to the oxidizing environment results in the growth of significant spectral intensity near 168.8 eV that is readily assigned to S^{6+},

likely in the form of sulfate. Although quantifying the relative magnitude of S^{6+} is difficult because of uncertainties in the surface structures and surface areas, it seems that the marcasite film may produce more S^{6+} than {100} pyrite. What can be asserted with more certainty is that the marcasite sample shows more significant oxidation of the S_2^{2-} group, as evidenced by the relatively large decrease in the 162.6-eV feature (due to emission from S_2^{2-}) and the growth of spectral intensity near 163.7 eV, with respect to pyrite {100}. More specifically, the ratio of the integrated area of reacted species (i.e., 168.8 and 163.7) to unreacted species (i.e., 162.6) for pyrite was found to be 1:2, whereas for the marcasite sample the ratio was 5:1. Intensity near 163.7 is consistent with the growth of S species with oxidation states greater than 1-, but the data cannot unambiguously identify the species. Polysulfide species exhibit intensity in this region, and prior XPS studies suggest that species such as thiosulfate can account for S 2p intensity near 163.4 eV (and 168.5 eV) (Guevremont et al., 1998a). Recent studies in our laboratory that used attenuated total reflectance Fourier transform infrared spectroscopy (data not shown) suggest that both thiosulfate and sulfate are present on the surface under our experimental conditions.

Data presented in Figure 5b also supports the increased reactivity of the marcasite film. The Fe 2p feature at 707.7 eV associated with Fe^{2+} in {100} pyrite and the marcasite thin film is markedly reduced, whereas spectral intensity near 711 eV, associated with Fe^{3+}oxidation products, is concomitantly increased after oxidation. The decrease in Fe^{2+} intensity is greater in the case of marcasite, suggesting that a larger fraction of the surface Fe^{2+} is oxidized to Fe^{3+} for this polymorph of FeS_2.

Increased reactivity of the marcasite film is not entirely unexpected because previous studies have suggested that marcasite is a more reactive mineral than pyrite (Rinker et al., 1997; Uhlig et al., 2001) in oxidizing environments. The reactivity of the marcasite thin film, however, brings forward the importance of short range order in mineral reactivity. At least, when discussing pyrite, nonstoichiometric defects such as Fe^{3+} and S^{2-} often are proposed as initial sites of oxidation (Guevremont et al., 1998a; Schaufuss et al., 1998a). Rupture of the *S*-S linkage during fracture of pyrite or marcasite, for example, can lead to the generation of such surface species (Schaufuss et al., 1998b). It might be speculated that such sites can lead to the generation of Fe^{3+} oxide product phases that have been proposed to contribute to pyrite oxidation (Eggleston et al., 1996). For the marcasite thin film discussed in this contribution, the contribution of S^{2-} to the surface reactivity was effectively removed. Although we cannot comment on the site density of Fe^{3+} on the thin film, we would expect it to be low, considering that S^{1-} is the only detectable S species in the film. The marcasite film, however, shows significant reactivity. This experimental observations suggests that long range order (such as crystallographic orientation) or short range defects, such as steps, kinks, etc., whose presence has been inferred from AFM, contributes significantly to the overall surface reactivity of marcasite (or presumably to pyrite). Such a conclusion is consistent with prior research from our laboratory that experimentally observed more significant oxidation on {111} pyrite than on {100} pyrite under identical oxidizing environments (Guevremont et al., 1998b), even though the site density of nonstoichiometric sites appeared to be similar. Research is presently being pursued in our laboratory to synthesize more well-defined thin films of marcasite and pyrite that will have less structural disorder.

4. SUMMARY

A thin film of marcasite has been investigated with XRD, AFM, synchrotron-based photoelectron spectroscopy, and XPS. The thin film presented a reproducible and atomically clean sample for surface science studies. AFM results suggest that the films are relatively uniform, but do expose a variety of sites at the surface. Synchrotron-based photoelectron spectroscopy, shows that the S 2p spectral region is dominated by emission from S_2^{2-} groups. Lesser S 2p contributions associated with surface shifted S_2^{2-} and polysulfides also are present. Concentration of the polysulfide impurity on the thin films appears to be significantly less than the same species on cleaved marcasite samples reported on in prior work in another laboratory. Even though the thin film had a low density of nonstoichiometric species, such as S^{2-}, it showed significant oxidation in a H_2O/O_2 environment. This results suggests that the presence of defects such as steps etc., inferred from AFM, dominated the surface reactivity.

Acknowledgments—D.R.S. and M.A.A.S. greatly appreciate support from the Department of Energy, Basic Energy Sciences, from grants DEFG0296ER14644 and DEFG029ER14633, respectively. Research was carried out in part at the National Synchrotron Light Source, Brookhaven National Laboratory, which is supported by the U.S. Department of Energy, Division of Materials Sciences, and Division of Chemical Sciences under contract DE-AC02-98CH10886. The Environmental Molecular Sciences Laboratory is operated by Pacific Northwest National Laboratory for the U.S. Department of Energy Office of Biologic and Environmental Research. Pacific Northwest National Laboratory is operated for the U.S. Department of Energy by Battelle Memorial Institute under contract DE-AC06-76RL0 1830. A.R.E. acknowledges support from the Temple University Francis H. Case and Daniel Swern Fellowships. We thank A. Celestian and J. Parise for conducting the X-ray diffractometry at SUNY-SB. We greatly appreciate the careful and thoughtful review by Dr. Wayne Nesbitt and an anonymous reviewer.

Associate editor: M. L. Machesky

REFERENCES

Bronold M., Kubala S., Pettenkofer C., and Jaegermann W. (1997) Thin pyrite (FeS_2) films by molecular beam deposition. *Thin Solid Films* **304,** 178–182.

Chambers S. A. (2000) Epitaxial growth and properties of thin film oxides. *Surf. Sci. Rep.* **39,** 105–180.

Chambers S. A., Thevuthasan S., and Joyce S. A. (2000) Surface structure of MBE-grown Fe_3O_4(001) by x-ray photoelectron diffraction and scanning tunneling microscopy. *Surf. Sci.* **450,** L273–L279.

Chusuei C. C., Lai X., Luo K., and Goodman D. W. (2001) Modeling heterogeneous catalysts: Metal clusters on planar oxide supports. *Top. Catal.* **14,** 71–83.

Eggleston C. M., Ehrhardt J., and Stumm W. A. M. (1996) Surface structural controls on pyrite oxidation kinetics: An XPS-UPS, STM and modeling study. *Am. Mineral.* **81,** 1036–1056.

Elsetinow A. R., Guevremont J. M., Strongin D. R., Schoonen M. A. A., and Strongin M. (2000) Oxidation of {100} and {111} surface of pyrite: Effects of preparation method. *Am. Mineral.* **85,** 623–626.

Ennaoui A., Fiechter S., Pettenkofer C., Alonso-Vante N., Bueker K., Bronold M., Hoepfner C., and Tributsch H. (1993) Iron disulfide for solar energy conversion. *Sol. Energy Mater. Sol. Cells.* **29,** 289–370.

Freund H. J., Ernst N., Risse T., Hamann H., and Rupprechter G. (2001) Models in heterogeneous catalysis: Surface science quo vadis? *Phys. Status Solidi A* **187,** 257–274.

Guevremont J., Bebié J., Strongin D. R., and Schoonen M. A. A. (1998a) Reactivity of the (100) plane of pyrite in oxidizing gaseous and aqueous environments: Effects of surface imperfections. *Environ. Sci. Technol.* **32,** 3743–3748.

Guevremont J. M., Elsetinow A. R., Strongin D. R., Bebie J., and Schoonen M. A. A. (1998b) Structure sensitivity of pyrite oxidation: Comparison of the (100) and (111) planes. *Am. Mineral.* **83(11–12, Pt. 1),** 1353–1356.

Heegeman W., Meister K. H., Betchold E., and Hayek K. (1975) The adsorption of sulfur on the (100) and (111) faces of platinium: A LEED and AES study. *Surface Sci.* **49,** 161–180.

Hoepfner C., Ellmer K., Ennaoui A., Pettenkofer C., Fiechter S., and Tributsch H. (1995) Stoichiometry-, phase- and orientation-controlled growth of polycrystalline pyrite (FeS_2) thin films by MOCVD. *J. Cryst. Growth* **151,** 325–34.

Hrbek J., Sham T. K., Shek M. -L., and Xu G. -Q. L. (1992) Potassium–oxygen interactions on a Ru(001) surface. *Langmuir* **8,** 2461–2472.

Kim Y. J., Gao Y., Herman G. S., Thevuthasan S., Jiang W., McCready D. E., and Chambers S. A. (1999) Growth and structure of epitaxial CeO_2 by oxygen-plasma–assisted molecular beam epitaxy. *J. Vac. Sci. Technol. A* **17,** 926–935.

Lodders K., Klingerhöffer G., and Kremser D. T. (1998) Chloritoid inclusions in pyrite from Navajún, Spain. *Can. Mineral.* **36,** 137–145.

Meester B., Reijnen L., Goossens A., and Schoonman J. (2000) Synthesis of pyrite (FeS_2) thin films by low-pressure MOCVD. *Chem. Vapor Deposition.* **6,** 121–128.

Rinker M. J., Nesbitt H. W., and Pratt A. R. (1997) Marcasite oxidation in low-temperature acidic (pH 3.0) solutions: Mechanism and rate laws. *Am. Mineral.* **82,** 900–912.

Rodriguez J. A. and Goodman D. W. (1995) Chemical and electronic properties of bimetallic surfaces. *Acc. Chem. Res.* **28,** 477–8.

Schaufuss A. G., Nesbitt H. W., Kartio I., Kartio I., Laajalehto K., Bancroft G. M., and Szargan R. (1998a) Incipient oxidation of fractured pyrite surfaces in air. *J. Electron Spectr. Related Phenomena* **96,** 69–82.

Schaufuss A. G., Nesbitt H. W., Kartio I., Laajalehto K., Bancroft G. M., and Szargan R. (1998b) Reactivity of surface chemical states on fractured pyrite. *Surf. Sci.* **411,** 321–328.

Somorjai G. A. (1981) *Chemistry in Two Dimensions: Surfaces* Cornel University Press, Ithica, NY.

Somorjai G. A. (1994) *Introduction to Surface Chemistry*. Wiley.

St. Clair T. P. and Goodman D. W. (2000) Metal nanoclusters supported on metal oxide thin films: Bridging the materials gap. *Top. Catal.* **13,** 5–19.

Thevuthasan S., Kim Y. J., Yi S. I., Chambers S. A., Morais J., Denecke R., Fadley C. S., Liu P., Kendelewicz T., and Brown Jr. G. E. (1999) Surface structure of MBE-grown α-Fe_2O_3(0001) by intermediate-energy x-ray photoelectron diffraction. *Surf. Sci.* **425,** 276–286.

Thomas B., Hopfner C., Ellmer K., Fiechter S., and Tributsch H. (1995) Growth of FeS_2 (pyrite) thin films on single crystalline substrates by low pressure metalorganic chemical vapour deposition. *J. Crystal Growth* **146,** 630–635.

Thomas B., Ellmer K., Muller C., Hopfner C., Fiechter S., and Tributsch H. (1997) Structural and photoelectrical properties of FeS_2 (pyrite) thin films grown by MOCVD. *J. Crystal Growth* **170,** 808–812.

Uhlig I., Szargan R., Nesbitt H. W., and Laajalehto K. (2001) Surface states and reactivity of pyrite and marcasite. *Appl. Surf. Sci.* **179,** 222–229.

Wagner C. (1953) Investigations on silver sulfide. *J. Phys. Chem.* **31,** 1819–1826.